

Search for Techniparticles in $e + \text{jets}$ Events at D0

V. M. Abazov,³⁵ B. Abbott,⁷⁵ M. Abolins,⁶⁵ B. S. Acharya,²⁸ M. Adams,⁵¹ T. Adams,⁴⁹ E. Aguilo,⁵ S. H. Ahn,³⁰ M. Ahsan,⁵⁹ G. D. Alexeev,³⁵ G. Alkhalaf,³⁹ A. Alton,^{64,*} G. Alverson,⁶³ G. A. Alves,² M. Anastasoiaie,³⁴ L. S. Ancu,³⁴ T. Andeen,⁵³ S. Anderson,⁴⁵ B. Andrieu,¹⁶ M. S. Anzels,⁵³ Y. Arnaud,¹³ M. Arov,⁵² A. Askew,⁴⁹ B. Åsman,⁴⁰ A. C. S. Assis Jesus,³ O. Atramentov,⁴⁹ C. Autermann,²⁰ C. Avila,⁷ C. Ay,²³ F. Badaud,¹² A. Baden,⁶¹ L. Bagby,⁵² B. Baldin,⁵⁰ D. V. Bandurin,⁵⁹ P. Banerjee,²⁸ S. Banerjee,²⁸ E. Barberis,⁶³ P. Bargassa,⁸⁰ P. Baringer,⁵⁸ C. Barnes,⁴³ J. Barreto,² J. F. Bartlett,⁵⁰ U. Bassler,¹⁶ D. Bauer,⁴³ S. Beale,⁵ A. Bean,⁵⁸ M. Begalli,³ M. Begel,⁷¹ C. Belanger-Champagne,⁴⁰ L. Bellantoni,⁵⁰ A. Bellavance,⁶⁷ J. A. Benitez,⁶⁵ S. B. Beri,²⁶ G. Bernardi,¹⁶ R. Bernhard,²² L. Berntzon,¹⁴ I. Bertram,⁴² M. Besançon,¹⁷ R. Beuselinck,⁴³ V. A. Bezzubov,³⁸ P. C. Bhat,⁵⁰ V. Bhatnagar,²⁶ M. Binder,²⁴ C. Biscarat,¹⁹ I. Blackler,⁴³ G. Blazey,⁵² F. Blekman,⁴³ S. Blessing,⁴⁹ D. Bloch,¹⁸ K. Bloom,⁶⁷ A. Boehnlein,⁵⁰ D. Boline,⁶² T. A. Bolton,⁵⁹ G. Borissov,⁴² K. Bos,³³ T. Bose,⁷⁷ A. Brandt,⁷⁸ R. Brock,⁶⁵ G. Brooijmans,⁷⁰ A. Bross,⁵⁰ D. Brown,⁷⁸ N. J. Buchanan,⁴⁹ D. Buchholz,⁵³ M. Buehler,⁸¹ V. Buescher,²² S. Burdin,⁵⁰ S. Burke,⁴⁵ T. H. Burnett,⁸² E. Busato,¹⁶ C. P. Buszello,⁴³ J. M. Butler,⁶² P. Calfayan,²⁴ S. Calvet,¹⁴ J. Cammin,⁷¹ S. Caron,³³ W. Carvalho,³ B. C. K. Casey,⁷⁷ N. M. Cason,⁵⁵ H. Castilla-Valdez,³² S. Chakrabarti,¹⁷ D. Chakraborty,⁵² K. M. Chan,⁷¹ A. Chandra,⁴⁸ F. Charles,¹⁸ E. Cheu,⁴⁵ F. Chevallier,¹³ D. K. Cho,⁶² S. Choi,³¹ B. Choudhary,²⁷ L. Christofek,⁷⁷ D. Claes,⁶⁷ B. Clément,¹⁸ C. Clément,⁴⁰ Y. Coadou,⁵ M. Cooke,⁸⁰ W. E. Cooper,⁵⁰ M. Corcoran,⁸⁰ F. Couderc,¹⁷ M.-C. Cousinou,¹⁴ B. Cox,⁴⁴ S. Crépe-Renaudin,¹³ D. Cutts,⁷⁷ M. Ćwiok,²⁹ H. da Motta,² A. Das,⁶² M. Das,⁶⁰ B. Davies,⁴² G. Davies,⁴³ K. De,⁷⁸ P. de Jong,³³ S. J. de Jong,³⁴ E. De La Cruz-Burelo,⁶⁴ C. De Oliveira Martins,³ J. D. Degenhardt,⁶⁴ F. Déliot,¹⁷ M. Demarteau,⁵⁰ R. Demina,⁷¹ D. Denisov,⁵⁰ S. P. Denisov,³⁸ S. Desai,⁵⁰ H. T. Diehl,⁵⁰ M. Diesburg,⁵⁰ M. Doidge,⁴² A. Dominguez,⁶⁷ H. Dong,⁷² L. V. Dudko,³⁷ L. Duflot,¹⁵ S. R. Dugad,²⁸ D. Duggan,⁴⁹ A. Duperrin,¹⁴ J. Dyer,⁶⁵ A. Dyshkant,⁵² M. Eads,⁶⁷ D. Edmunds,⁶⁵ J. Ellison,⁴⁸ V. D. Elvira,⁵⁰ Y. Enari,⁷⁷ S. Eno,⁶¹ P. Ermolov,³⁷ H. Evans,⁵⁴ A. Evdokimov,³⁶ V. N. Evdokimov,³⁸ L. Feligioni,⁶² A. V. Ferapontov,⁵⁹ T. Ferbel,⁷¹ F. Fiedler,²⁴ F. Filthaut,³⁴ W. Fisher,⁵⁰ H. E. Fisk,⁵⁰ M. Ford,⁴⁴ M. Fortner,⁵² H. Fox,²² S. Fu,⁵⁰ S. Fuess,⁵⁰ T. Gadfort,⁸² C. F. Galea,³⁴ E. Gallas,⁵⁰ E. Galyaev,⁵⁵ C. Garcia,⁷¹ A. Garcia-Bellido,⁸² V. Gavrilov,³⁶ A. Gay,¹⁸ P. Gay,¹² W. Geist,¹⁸ D. Gelé,¹⁸ R. Gelhaus,⁴⁸ C. E. Gerber,⁵¹ Y. Gershtein,⁴⁹ D. Gillberg,⁵ G. Ginter,⁷¹ N. Gollub,⁴⁰ B. Gómez,⁷ A. Goussiou,⁵⁵ P. D. Grannis,⁷² H. Greenlee,⁵⁰ Z. D. Greenwood,⁶⁰ E. M. Gregores,⁴ G. Grenier,¹⁹ Ph. Gris,¹² J.-F. Grivaz,¹⁵ A. Grohsjean,²⁴ S. Grünendahl,⁵⁰ M. W. Grünewald,²⁹ F. Guo,⁷² J. Guo,⁷² G. Gutierrez,⁵⁰ P. Gutierrez,⁷⁵ A. Haas,⁷⁰ N. J. Hadley,⁶¹ P. Haefner,²⁴ S. Hagopian,⁴⁹ J. Haley,⁶⁸ I. Hall,⁷⁵ R. E. Hall,⁴⁷ L. Han,⁶ K. Hanagaki,⁵⁰ P. Hansson,⁴⁰ K. Harder,⁴⁴ A. Harel,⁷¹ R. Harrington,⁶³ J. M. Hauptman,⁵⁷ R. Hauser,⁶⁵ J. Hays,⁴³ T. Hebbeker,²⁰ D. Hedin,⁵² J. G. Hegeman,³³ J. M. Heinmiller,⁵¹ A. P. Heinson,⁴⁸ U. Heintz,⁶² C. Hensel,⁵⁸ K. Herner,⁷² G. Hesketh,⁶³ M. D. Hildreth,⁵⁵ R. Hirosky,⁸¹ J. D. Hobbs,⁷² B. Hoeneisen,¹¹ H. Hoeth,²⁵ M. Hohlfield,¹⁵ S. J. Hong,³⁰ R. Hooper,⁷⁷ P. Houben,³³ Y. Hu,⁷² Z. Hubacek,⁹ V. Hynek,⁸ I. Iashvili,⁶⁹ R. Illingworth,⁵⁰ A. S. Ito,⁵⁰ S. Jabeen,⁶² M. Jaffré,¹⁵ S. Jain,⁷⁵ K. Jakobs,²² C. Jarvis,⁶¹ A. Jenkins,⁴³ R. Jesik,⁴³ K. Johns,⁴⁵ C. Johnson,⁷⁰ M. Johnson,⁵⁰ A. Jonckheere,⁵⁰ P. Jonsson,⁴³ A. Juste,⁵⁰ D. Käfer,²⁰ S. Kahn,⁷³ E. Kajfasz,¹⁴ A. M. Kalinin,³⁵ J. M. Kalk,⁶⁰ J. R. Kalk,⁶⁵ S. Kappler,²⁰ D. Karmanov,³⁷ J. Kasper,⁶² P. Kasper,⁵⁰ I. Katsanos,⁷⁰ D. Kau,⁴⁹ R. Kaur,²⁶ R. Kehoe,⁷⁹ S. Kermiche,¹⁴ N. Khalatyan,⁶² A. Khanov,⁷⁶ A. Kharchilava,⁶⁹ Y. M. Kharzheev,³⁵ D. Khatidze,⁷⁰ H. Kim,³¹ T. J. Kim,³⁰ M. H. Kirby,³⁴ B. Klima,⁵⁰ J. M. Kohli,²⁶ J.-P. Konrath,²² M. Kopal,⁷⁵ V. M. Korablev,³⁸ J. Kotcher,⁷³ B. Kothari,⁷⁰ A. Koubarovsky,³⁷ A. V. Kozelov,³⁸ D. Krop,⁵⁴ A. Kryemadhi,⁸¹ T. Kuhl,²³ A. Kumar,⁶⁹ S. Kunori,⁶¹ A. Kupco,¹⁰ T. Kurča,¹⁹ J. Kvita,⁸ D. Lam,⁵⁵ S. Lammers,⁷⁰ G. Landsberg,⁷⁷ J. Lazoflores,⁴⁹ A.-C. Le Bihan,¹⁸ P. Lebrun,¹⁹ W. M. Lee,⁵⁰ A. Leflat,³⁷ F. Lehner,⁴¹ V. Lesne,¹² J. Leveque,⁴⁵ P. Lewis,⁴³ J. Li,⁷⁸ L. Li,⁴⁸ Q. Z. Li,⁵⁰ S. M. Lietti,⁴ J. G. R. Lima,⁵² D. Lincoln,⁵⁰ J. Linnemann,⁶⁵ V. V. Lipaev,³⁸ R. Lipton,⁵⁰ Z. Liu,⁵ L. Lobo,⁴³ A. Lobodenko,³⁹ M. Lokajicek,¹⁰ A. Lounis,¹⁸ P. Love,⁴² H. J. Lubatti,⁸² M. Lynker,⁵⁵ A. L. Lyon,⁵⁰ A. K. A. Maciel,² R. J. Madaras,⁴⁶ P. Mättig,²⁵ C. Magass,²⁰ A. Magerkurth,⁶⁴ N. Makovec,¹⁵ P. K. Mal,⁵⁵ H. B. Malbouisson,³ S. Malik,⁶⁷ V. L. Malyshev,³⁵ H. S. Mao,⁵⁰ Y. Maravin,⁵⁹ R. McCarthy,⁷² A. Melnitchouk,⁶⁶ A. Mendes,¹⁴ L. Mendoza,⁷ P. G. Mercadante,⁴ M. Merkin,³⁷ K. W. Merritt,⁵⁰ A. Meyer,²⁰ J. Meyer,²¹ M. Michaut,¹⁷ H. Miettinen,⁸⁰ T. Millet,¹⁹ J. Mitrevski,⁷⁰ J. Molina,³ R. K. Mommsen,⁴⁴ N. K. Mondal,²⁸ J. Monk,⁴⁴ R. W. Moore,⁵ T. Moulík,⁵⁸ G. S. Muanza,¹⁹ M. Mulders,⁵⁰ M. Mulhearn,⁷⁰ O. Mundal,²² L. Mundim,³ E. Nagy,¹⁴ M. Naimuddin,²⁷ M. Narain,⁶² N. A. Naumann,³⁴ H. A. Neal,⁶⁴ J. P. Negret,⁷ P. Neustroev,³⁹ C. Noeding,²² A. Nomerotski,⁵⁰ S. F. Novaes,⁴ T. Nunnemann,²⁴ V. O'Dell,⁵⁰ D. C. O'Neil,⁵ G. Obrant,³⁹ C. Ochando,¹⁵ V. Oguri,³ N. Oliveira,³ D. Onoprienko,⁵⁹ N. Oshima,⁵⁰ J. Osta,⁵⁵ R. Otec,⁹ G. J. Otero y Garzón,⁵¹ M. Owen,⁴⁴ P. Padley,⁸⁰ M. Pangilinan,⁶² N. Parashar,⁵⁶

S.-J. Park,⁷¹ S. K. Park,³⁰ J. Parsons,⁷⁰ R. Partridge,⁷⁷ N. Parua,⁷² A. Patwa,⁷³ G. Pawloski,⁸⁰ P. M. Perea,⁴⁸ K. Peters,⁴⁴ Y. Peters,²⁵ P. Pétrouff,¹⁵ M. Petteni,⁴³ R. Piegaiia,¹ J. Piper,⁶⁵ M.-A. Pleier,²¹ P. L. M. Podesta-Lerma,³² V. M. Podstavkov,⁵⁰ Y. Pogorelov,⁵⁵ M.-E. Pol,² A. Pompoš,⁷⁵ B. G. Pope,⁶⁵ A. V. Popov,³⁸ C. Potter,⁵ W. L. Prado da Silva,³ H. B. Prosper,⁴⁹ S. Protopopescu,⁷³ J. Qian,⁶⁴ A. Quadt,²¹ B. Quinn,⁶⁶ M. S. Rangel,² K. J. Rani,²⁸ K. Ranjan,²⁷ P. N. Ratoff,⁴² P. Renkel,⁷⁹ S. Reucroft,⁶³ M. Rijssenbeek,⁷² I. Ripp-Baudot,¹⁸ F. Rizatdinova,⁷⁶ S. Robinson,⁴³ R. F. Rodrigues,³ C. Royon,¹⁷ P. Rubinov,⁵⁰ R. Ruchti,⁵⁵ G. Sajot,¹³ A. Sánchez-Hernández,³² M. P. Sanders,¹⁶ A. Santoro,³ G. Savage,⁵⁰ L. Sawyer,⁶⁰ T. Scanlon,⁴³ D. Schaile,²⁴ R. D. Schamberger,⁷² Y. Scheglov,³⁹ H. Schellman,⁵³ P. Schieferdecker,²⁴ C. Schmitt,²⁵ C. Schwanenberger,⁴⁴ A. Schwartzman,⁶⁸ R. Schwienhorst,⁶⁵ J. Sekaric,⁴⁹ S. Sengupta,⁴⁹ H. Severini,⁷⁵ E. Shabalina,⁵¹ M. Shamim,⁵⁹ V. Shary,¹⁷ A. A. Shchukin,³⁸ R. K. Shivpuri,²⁷ D. Shpakov,⁵⁰ V. Siccaldi,¹⁸ R. A. Sidwell,⁵⁹ V. Simak,⁹ V. Sirotenko,⁵⁰ P. Skubic,⁷⁵ P. Slattey,⁷¹ R. P. Smith,⁵⁰ G. R. Snow,⁶⁷ J. Snow,⁷⁴ S. Snyder,⁷³ S. Söldner-Rembold,⁴⁴ X. Song,⁵² L. Sonnenschein,¹⁶ A. Sopczak,⁴² M. Sosebee,⁷⁸ K. Soustruznik,⁸ M. Souza,² B. Spurlock,⁷⁸ J. Stark,¹³ J. Steele,⁶⁰ V. Stolin,³⁶ A. Stone,⁵¹ D. A. Stoyanova,³⁸ J. Strandberg,⁶⁴ S. Strandberg,⁴⁰ M. A. Strang,⁶⁹ M. Strauss,⁷⁵ R. Ströhmer,²⁴ D. Strom,⁵³ M. Strovink,⁴⁶ L. Stutte,⁵⁰ S. Sumowidagdo,⁴⁹ P. Svoisky,⁵⁵ A. Sznajder,³ M. Talby,¹⁴ P. Tamburello,⁴⁵ W. Taylor,⁵ P. Telford,⁴⁴ J. Temple,⁴⁵ B. Tiller,²⁴ M. Titov,²² V. V. Tokmenin,³⁵ M. Tomoto,⁵⁰ T. Toole,⁶¹ I. Torchiani,²² T. Trefzger,²³ S. Trincaz-Duvoid,¹⁶ D. Tsybychev,⁷² B. Tuchming,¹⁷ C. Tully,⁶⁸ P. M. Tuts,⁷⁰ R. Unalan,⁶⁵ L. Uvarov,³⁹ S. Uvarov,³⁹ S. Uzunyan,⁵² B. Vachon,⁵ P. J. van den Berg,³³ B. van Eijk,³⁵ R. Van Kooten,⁵⁴ W. M. van Leeuwen,³³ N. Varelas,⁵¹ E. W. Varnes,⁴⁵ A. Vartapetian,⁷⁸ I. A. Vasilyev,³⁸ M. Vaupel,²⁵ P. Verdier,¹⁹ L. S. Vertogradov,³⁵ M. Verzocchi,⁵⁰ F. Villeneuve-Seguiier,⁴³ P. Vint,⁴³ J.-R. Vlimant,¹⁶ E. Von Toerne,⁵⁹ M. Voutilainen,^{67,†} M. Vreeswijk,³³ H. D. Wahl,⁴⁹ L. Wang,⁶¹ M. H. L. S. Wang,⁵⁰ J. Warchol,⁵⁵ G. Watts,⁸² M. Wayne,⁵⁵ G. Weber,²³ M. Weber,⁵⁰ H. Weerts,⁶⁵ N. Wermes,²¹ M. Wetstein,⁶¹ A. White,⁷⁸ D. Wicke,²⁵ G. W. Wilson,⁵⁸ S. J. Wimpenny,⁴⁸ M. Wobisch,⁵⁰ J. Womersley,⁵⁰ D. R. Wood,⁶³ T. R. Wyatt,⁴⁴ Y. Xie,⁷⁷ S. Yacoob,⁵³ R. Yamada,⁵⁰ M. Yan,⁶¹ T. Yasuda,⁵⁰ Y. A. Yatsunenko,³⁵ K. Yip,⁷³ H. D. Yoo,⁷⁷ S. W. Youn,⁵³ C. Yu,¹³ J. Yu,⁷⁸ A. Yurkewicz,⁷² A. Zatserklyaniy,⁵² C. Zeitnitz,²⁵ D. Zhang,⁵⁰ T. Zhao,⁸² B. Zhou,⁶⁴ J. Zhu,⁷² M. Zielinski,⁷¹ D. Zieminska,⁵⁴ A. Zieminski,⁵⁴ V. Zutshi,⁵² and E. G. Zverev³⁷

(D0 Collaboration)

¹Universidad de Buenos Aires, Buenos Aires, Argentina²LAFEX, Centro Brasileiro de Pesquisas Físicas, Rio de Janeiro, Brazil³Universidade do Estado do Rio de Janeiro, Rio de Janeiro, Brazil⁴Instituto de Física Teórica, Universidade Estadual Paulista, São Paulo, Brazil⁵University of Alberta, Edmonton, Alberta, Canada,

Simon Fraser University, Burnaby, British Columbia, Canada,

York University, Toronto, Ontario, Canada,

and McGill University, Montreal, Quebec, Canada

⁶University of Science and Technology of China, Hefei, People's Republic of China⁷Universidad de los Andes, Bogotá, Colombia⁸Center for Particle Physics, Charles University, Prague, Czech Republic⁹Czech Technical University, Prague, Czech Republic¹⁰Center for Particle Physics, Institute of Physics, Academy of Sciences of the Czech Republic, Prague, Czech Republic¹¹Universidad San Francisco de Quito, Quito, Ecuador¹²Laboratoire de Physique Corpusculaire, IN2P3-CNRS, Université Blaise Pascal, Clermont-Ferrand, France¹³Laboratoire de Physique Subatomique et de Cosmologie, IN2P3-CNRS, Université de Grenoble I, Grenoble, France¹⁴CPPM, IN2P3-CNRS, Université de la Méditerranée, Marseille, France¹⁵Laboratoire de l'Accélérateur Linéaire, IN2P3-CNRS et Université Paris-Sud, Orsay, France¹⁶LPNHE, IN2P3-CNRS, Universités Paris VI and VII, Paris, France¹⁷DAPNIA/Service de Physique des Particules, CEA, Saclay, France¹⁸IPHC, IN2P3-CNRS, Université Louis Pasteur, Strasbourg, France, and Université de Haute Alsace, Mulhouse, France¹⁹Institut de Physique Nucléaire de Lyon, IN2P3-CNRS, Université Claude Bernard, Villeurbanne, France²⁰III. Physikalisches Institut A, RWTH Aachen, Aachen, Germany²¹Physikalisches Institut, Universität Bonn, Bonn, Germany²²Physikalisches Institut, Universität Freiburg, Freiburg, Germany²³Institut für Physik, Universität Mainz, Mainz, Germany²⁴Ludwig-Maximilians-Universität München, München, Germany²⁵Fachbereich Physik, University of Wuppertal, Wuppertal, Germany²⁶Panjab University, Chandigarh, India

- ²⁷Delhi University, Delhi, India
²⁸Tata Institute of Fundamental Research, Mumbai, India
²⁹University College Dublin, Dublin, Ireland
³⁰Korea Detector Laboratory, Korea University, Seoul, Korea
³¹SungKyunKwan University, Suwon, Korea
³²CINVESTAV, Mexico City, Mexico
³³FOM-Institute NIKHEF and University of Amsterdam/NIKHEF, Amsterdam, The Netherlands
³⁴Radboud University Nijmegen/NIKHEF, Nijmegen, The Netherlands
³⁵Joint Institute for Nuclear Research, Dubna, Russia
³⁶Institute for Theoretical and Experimental Physics, Moscow, Russia
³⁷Moscow State University, Moscow, Russia
³⁸Institute for High Energy Physics, Protvino, Russia
³⁹Petersburg Nuclear Physics Institute, St. Petersburg, Russia
⁴⁰Lund University, Lund, Sweden, Royal Institute of Technology and Stockholm University, Stockholm, Sweden, and Uppsala University, Uppsala, Sweden
⁴¹Physik Institut der Universität Zürich, Zürich, Switzerland
⁴²Lancaster University, Lancaster, United Kingdom
⁴³Imperial College, London, United Kingdom
⁴⁴University of Manchester, Manchester, United Kingdom
⁴⁵University of Arizona, Tucson, Arizona 85721, USA
⁴⁶Lawrence Berkeley National Laboratory and University of California, Berkeley, California 94720, USA
⁴⁷California State University, Fresno, California 93740, USA
⁴⁸University of California, Riverside, California 92521, USA
⁴⁹Florida State University, Tallahassee, Florida 32306, USA
⁵⁰Fermi National Accelerator Laboratory, Batavia, Illinois 60510, USA
⁵¹University of Illinois at Chicago, Chicago, Illinois 60607, USA
⁵²Northern Illinois University, DeKalb, Illinois 60115, USA
⁵³Northwestern University, Evanston, Illinois 60208, USA
⁵⁴Indiana University, Bloomington, Indiana 47405, USA
⁵⁵University of Notre Dame, Notre Dame, Indiana 46556, USA
⁵⁶Purdue University Calumet, Hammond, Indiana 46323, USA
⁵⁷Iowa State University, Ames, Iowa 50011, USA
⁵⁸University of Kansas, Lawrence, Kansas 66045, USA
⁵⁹Kansas State University, Manhattan, Kansas 66506, USA
⁶⁰Louisiana Tech University, Ruston, Louisiana 71272, USA
⁶¹University of Maryland, College Park, Maryland 20742, USA
⁶²Boston University, Boston, Massachusetts 02215, USA
⁶³Northeastern University, Boston, Massachusetts 02115, USA
⁶⁴University of Michigan, Ann Arbor, Michigan 48109, USA
⁶⁵Michigan State University, East Lansing, Michigan 48824, USA
⁶⁶University of Mississippi, University, Mississippi 38677, USA
⁶⁷University of Nebraska, Lincoln, Nebraska 68588, USA
⁶⁸Princeton University, Princeton, New Jersey 08544, USA
⁶⁹State University of New York, Buffalo, New York 14260, USA
⁷⁰Columbia University, New York, New York 10027, USA
⁷¹University of Rochester, Rochester, New York 14627, USA
⁷²State University of New York, Stony Brook, New York 11794, USA
⁷³Brookhaven National Laboratory, Upton, New York 11973, USA
⁷⁴Langston University, Langston, Oklahoma 73050, USA
⁷⁵University of Oklahoma, Norman, Oklahoma 73019, USA
⁷⁶Oklahoma State University, Stillwater, Oklahoma 74078, USA
⁷⁷Brown University, Providence, Rhode Island 02912, USA
⁷⁸University of Texas, Arlington, Texas 76019, USA
⁷⁹Southern Methodist University, Dallas, Texas 75275, USA
⁸⁰Rice University, Houston, Texas 77005, USA
⁸¹University of Virginia, Charlottesville, Virginia 22901, USA
⁸²University of Washington, Seattle, Washington 98195, USA

(Received 8 December 2006; published 31 May 2007)

We search for the technicolor process $p\bar{p} \rightarrow \rho_T/\omega_T \rightarrow W\pi_T$ in events containing one electron and two jets, in data corresponding to an integrated luminosity of 390 pb^{-1} , recorded by the D0 experiment at the

Fermilab Tevatron. Technicolor predicts that technipions π_T decay dominantly into $b\bar{b}$, $b\bar{c}$, or $\bar{b}c$, depending on their charge. In these events b and c quarks are identified by their secondary decay vertices within jets. Two analysis methods based on topological variables are presented. Since no excess above the standard model prediction was found, the result is presented as an exclusion in the π_T vs ρ_T mass plane for a given set of model parameters.

DOI: [10.1103/PhysRevLett.98.221801](https://doi.org/10.1103/PhysRevLett.98.221801)

PACS numbers: 12.60.Nz, 13.85.Rm

Technicolor (TC), first formulated by Weinberg and Susskind [1,2], provides a dynamical explanation of electroweak symmetry breaking through a new strong $SU(N_{TC})$ gauge interaction acting on new fermions, called “technifermions.” TC is a non-Abelian gauge theory modeled after quantum chromodynamics (QCD). In its low-energy limit, a spontaneous breaking of the global chiral symmetry in the technifermion sector leads to electroweak symmetry breaking. The Nambu-Goldstone bosons produced in this process are called technipions π_T , in analogy with the pions of QCD. Three of these technipions become the longitudinal components of the W and Z bosons, making them massive. An additional gauge interaction, called extended TC [3], couples standard model (SM) fermions and technifermions to provide a mechanism for generating quark and lepton masses.

Extensions of the basic TC model tend to require the number N_D of technifermion doublets to be large. In general, the TC scale $\Lambda_{TC} \approx O(1) \times F_{TC}$, where F_{TC} is the technipion decay constant, depends inversely on the number of technifermion doublets: $F_{TC} \approx 246 \text{ GeV} / \sqrt{N_D}$. For large N_D , the lowest lying technihadrons have masses on the order of a few hundred giga-electron-volts. This scenario is referred to as low-scale TC [4]. Low-scale TC models predict the existence of scalar technimesons, π_T^\pm and π_T^0 , and vector technimesons, ρ_T and ω_T .

General features of low-scale TC have been summarized in the TC strawman model [5,6]. The analysis presented in this Letter is based on Ref. [6]. Previous searches [7] for TC have been carried out by CDF and DELPHI experiments. Because of changes in the model, they cannot be directly compared to the results presented in this Letter. The previous CDF result was based on Ref. [4] which did not consider the decay $\rho_T/\omega_T \rightarrow G\pi_T$, where G is a transversely polarized electroweak gauge boson (γ , Z^0 , or W^\pm). Inclusion of this decay in Refs. [5,6] leads to a decrease in the $\rho \rightarrow W\pi_T$ rate. The DELPHI experiment used Ref. [5] in which the cross sections, while appropriate for narrow ρ_T production in $\bar{q}q$ collisions, are incorrect for off-resonance production in e^+e^- collisions such as at LEP (see Ref. [8]).

Vector technimesons are expected to be produced with substantial rates at the Fermilab Tevatron Collider via the Drell-Yan-like electroweak process $p\bar{p} \rightarrow \rho_T + X$ or $\omega_T + X$. They decay to a gauge boson (γ , W , Z) and a technipion or to fermion-antifermion pairs. The production cross sections and branching fractions depend on the masses of the vector technimesons, $M(\rho_T)$ and $M(\omega_T)$,

on the TC charges of the technifermions, on the mass differences between the vector and scalar technimesons, which determine the spectrum of accessible decay channels, and on two mass parameters, M_A for axial-vector and M_V for vector couplings. The parameter M_V controls the rate for the decay ρ_T , $\omega_T \rightarrow \gamma + \pi_T$ and is unknown *a priori*. Scaling from the QCD decay ρ , $\omega \rightarrow \gamma + \pi^0$, the authors of Ref. [6] suggest a value of several hundred giga-electron-volts. We set $M_A = M_V$, and evaluate the production and decay rates at two different values: 100 and 500 GeV. For all other parameters, we use the default values quoted in Table III of Ref. [6]. The cross sections for ρ_T and π_T production at the Tevatron in the mass range of a few hundred giga-electron-volts are expected to be in the range of 2 to 10 pb. Technipion coupling to the SM particles is proportional to their masses, and thus they predominantly decay into $b\bar{b}$, $b\bar{c}$, or $\bar{b}c$, depending on their charge.

In this Letter, we describe a search for the decay of vector technimesons to $W\pi_T$, followed by the decays $W \rightarrow e\nu$ and $\pi_T \rightarrow b\bar{b}$, $b\bar{c}$, or $c\bar{b}$. In the D0 detector, which is described in detail in Ref. [9], the signature of this process is an isolated electron and missing transverse momentum (\cancel{p}_T) from the undetected neutrino from the decay of the W boson, and two jets of hadrons coming from the fragmentation of the quarks from the decay of the technipion. Jets are reconstructed using the run II cone algorithm [10] with a cone size of 0.5. We search for events with this signature in the data collected with a single electron trigger until July 2004 and corresponding to an integrated luminosity of $388 \pm 25 \text{ pb}^{-1}$ [11].

There are a number of SM processes that can result in the same final state signature as $W\pi_T$ production. Vector boson production in association with jets is the dominant background. Z boson production can be suppressed by vetoing on a second electron and requiring significant \cancel{p}_T . Most of the jets in $W + \text{jets}$ events originate from the fragmentation of light quarks or gluons and therefore requiring the explicit identification of at least one jet from the fragmentation of a b or c quark suppresses this background, leaving only $W + b\bar{b}$, $W + b$, $W + c\bar{c}$, and $W + c$ events. Top-antitop pair production, followed by the decay to $t \rightarrow e\nu b$, is another background. It has an additional lepton, or three jets from the second top quark, and can be reduced by selecting events with exactly two jets. Single top quark production is an irreducible background, but it has a smaller cross section. We simulate all these processes using either PYTHIA [12] or ALPGEN [13]

Monte Carlo (MC) generators, followed by the D0 detector simulation based on GEANT [14]. Quark hadronization and fragmentation is simulated using PYTHIA.

The multijet background is due to events with poorly measured jets, resulting in missing momentum and a jet that is misidentified as an electron. Background from the mistagged $W + \text{jets}$ process originates from events in which a light-quark or gluon jet is incorrectly identified as a b jet. These instrumental background contributions are estimated from the same data sample before requiring the identification of a b jet.

We select events in which there is exactly one well-identified electron based on tracking and calorimeter data with transverse momentum $p_T > 20$ GeV and pseudorapidity $|\eta| < 1.1$ [$\eta = -\ln[\tan(\theta/2)]$, θ is the polar angle with respect to the proton beam]. There must be significant \cancel{p}_T , measured in two ways: $\cancel{p}_T^{\text{obj}} > 20$ GeV computed as the negative sum of the jet momentum vectors and the electron momentum vector and $\cancel{p}_T > 20$ GeV which also includes the calorimeter energy deposit not assigned to the electron or the jets. We require the transverse mass $M_T(e\nu) > 30$ GeV. We further require the presence of exactly two jets with $p_T > 20$ GeV and $|\eta| < 2.5$.

To further reduce backgrounds, we take advantage of the long lifetime of b flavored hadrons. Tracks from the decay products of b hadrons may not project back to the proton-antiproton collision, but have a significant impact parameter. Any pair of tracks, with distance of closest approach d between the track and the beam line divided by its uncertainty $d/\sigma(d) > 3$, is used as a seed for secondary vertices [15]. Additional tracks are attached iteratively to the seed vertices if their χ^2 contribution to the vertex fit is consistent with originating from the vertex. A jet is considered b tagged when there is at least one secondary vertex, with a decay length projected into the plane transverse to the beam line (L_{xy}) divided by its uncertainty $L_{xy}/\sigma(L_{xy}) > 7$ within $\Delta\mathcal{R} = \sqrt{(\Delta\eta)^2 + (\Delta\phi)^2} < 0.5$ of the jet axis. We require at least one jet to be b tagged. This leaves us with 117 events in our final data sample.

The expected background event yields are listed in Table I. When estimating these yields, each MC event is weighted by the probability that at least one jet is tagged as a b jet. The tagging probability is parametrized as a function of jet flavor, jet p_T , and η . The efficiency of tagging a jet from the fragmentation of a b quark is derived from collider data which were enriched in their b jet contents by requiring a muon to be reconstructed within at least one jet to preferentially select jets with semileptonic b decays. The probability of tagging a c jet is derived from the tagging probability for b jets by multiplying by the ratio of tagging probabilities for c and b jets derived from MC simulations. We derive the probability to tag a light-quark or gluon jet from a set of dijet events, corrected for contamination by c and b jets. The MC events are also weighted by the ratios of jet and electron finding efficien-

TABLE I. Number of events observed in the data and expected from signal and background sources after the kinematic selection; only statistical errors are reported. For the expected number of signal events quoted we assume $M(\rho_T) = 210$ GeV and $M(\pi_T) = 110$ GeV.

Final data sample	117
Signal	
$\rho_T/\omega_T \rightarrow W + \pi_T \rightarrow e\nu b\bar{b}$ ($M_V = 100$ GeV)	11.1 ± 0.1
$\rho_T/\omega_T \rightarrow W + \pi_T \rightarrow e\nu b\bar{b}$ ($M_V = 500$ GeV)	17.1 ± 0.2
Physics background	
$t\bar{t} \rightarrow \ell\nu b q\bar{q} b$	7.9 ± 0.5
$t\bar{t} \rightarrow \ell^+ \nu b \ell^- \nu\bar{b}$	14.1 ± 0.3
$W^* \rightarrow tb \rightarrow e\nu b\bar{b}$ or $\tau\nu b\bar{b}$	3.5 ± 0.1
$tqb \rightarrow e\nu b\bar{b}$ or $\tau\nu b\bar{b}$	4.3 ± 0.1
$W(\rightarrow e\nu) + \text{heavy flavor}$	56.4 ± 4.2
$WZ \rightarrow e\nu b\bar{b}$	1.10 ± 0.02
$Z(\rightarrow e^+e^-)$	0.5 ± 0.4
$Z(\rightarrow e^+e^-) + b\bar{b}$	0.60 ± 0.03
Instrumental background	
Multijet events	16.3 ± 3.2
Mistagged $W(\rightarrow e\nu) + \text{jets}$	10.3 ± 0.3
Total background	115.1 ± 5.4

cies in MC and collider data. Electron finding efficiencies are measured in $Z \rightarrow ee$ events in both data and MC simulations.

We use the PYTHIA event generator to simulate signal events, modeling initial state and final state radiation, fragmentation, and hadronization. To generate $W\pi_T$ signal events for a range of values of the technimeson masses, we use a fast, parametrized detector simulation that was tuned to reproduce the kinematic distributions and acceptances from events simulated with the detailed GEANT-based detector simulation. For the cross section calculations, CTEQ5L [16] parton distribution functions are used. Finally, as is appropriate for this Drell-Yan-like process, the cross section is multiplied by a K factor of 1.3 to approximate next-to-leading order contributions to the cross section [17]. We generate events with ρ_T masses from 160 to 220 GeV and assume $M(\omega_T) = M(\rho_T)$. The π_T mass values start at the kinematic threshold for $W\pi_T$ production at $M(\pi_T) = M(\rho_T) - M(W)$ and go down to $M(\pi_T) = M(\rho_T)/2 - 5$ GeV where the decay channel $\rho_T^{\pm(0)} \rightarrow \pi_T^{\pm(0,\pm)} \pi_T^{0(0,\mp)}$ is accessible, reducing the branching fraction of $\rho_T^{\pm(0)} \rightarrow W\pi_T$.

At this point our data sample is still dominated by background. We therefore use additional variables that characterize the topology of the events to discriminate between signal and background. These variables are the azimuthal angle difference between the two jets $\Delta\phi(j, j)$, the azimuthal angle difference between the electron and the \cancel{p}_T , $\Delta\phi(e, \cancel{p}_T)$, the transverse momentum of the dijet system $p_T(jj)$, the scalar sum of the transverse momenta of

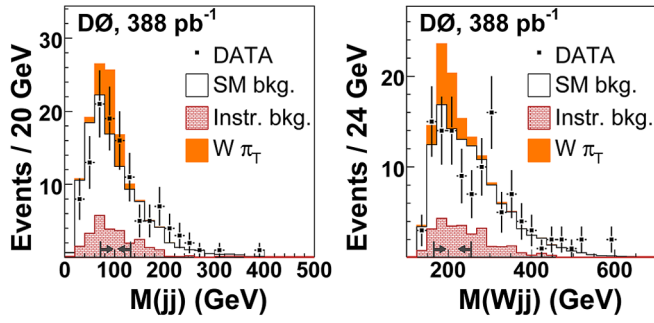


FIG. 1 (color online). Distributions of $M(jj)$ and $M(Wjj)$ after final kinematic selection. The $W\pi_T$ signal is shown for $M(\rho_T) = 210$ GeV and $M(\pi_T) = 110$ GeV. Arrows at the bottom indicate the cuts applied in the cut-based analysis for the signal mass point shown.

the electron and the two jets H_T^e , the invariant mass of the dijet system $M(jj)$, and the invariant mass of the W boson-dijet system $M(Wjj)$. The TC particles are expected to have narrow widths (≈ 1 GeV). We should therefore see enhancements in the distributions of $M(jj)$ and $M(Wjj)$, consistent in width with the detector resolution. $M(jj)$, corresponding to the reconstructed π_T mass, and $M(Wjj)$, corresponding to the reconstructed ρ_T mass, are shown in Fig. 1. We reconstruct the W boson from the electron and the missing transverse momentum using the W boson mass constraint to solve for p_z of the neutrino. If there are two real solutions, we take the smaller value of neutrino $|p_z|$. If there is only a complex solution, we take the real part. We use two approaches to separate signal and background, a cut-based analysis and a neural network (NN) analysis.

The cut-based analysis is optimized using MC simulations to maximize the ratio S/\sqrt{B} for every set of technimeson mass values. S is the expected number of $W\pi_T$ events and B is the expected number of background events. For each topological variable, the S/\sqrt{B} ratio is evaluated

as a function of the value of the variable to determine a set of lower, upper, or window cuts which maximizes this ratio. The NN analysis uses the topological variables H_T^e , $\Delta\phi(e, \not{p}_T)$, $\Delta\phi(jj)$, $p_T(jj)$, the transverse momenta of both jets and of the electron and \not{p}_T . A two-stage NN based on the multilayer perceptron algorithm [18] is used. The first stage consists of three independent networks which are trained to reject the three main backgrounds, top quark production, $W + b\bar{b}$ production, and all other $W +$ jets production including heavy flavors. Each of these three networks has eight input nodes and one hidden layer with 24 nodes. The second stage network has three input nodes, connected to the outputs of the three networks in the first stage, and one hidden layer with six nodes. The second stage network is trained using all nine physics background processes. The networks are trained separately for each set of TC mass values. We then apply the trained neural networks to the collider data, TC signals, and physics and instrumental backgrounds to obtain the discriminator output spectra. We optimize the discriminator cut for every set of techniparticle masses to maximize S/\sqrt{B} .

In Table II, we list the number of observed events, the background estimation, and the signal expectation for both analysis techniques. The data presented in this table are after all cuts for the cut-based analysis and with a loose cut on NN discriminant for the NN analysis. We note that there is no excess in our data over the expected background. We compute upper limits on the $\rho_T \rightarrow W\pi_T \rightarrow e\nu b\bar{b}(\bar{c})$ production cross section times branching fraction. The uncertainties in the background event yields total to 10%–12% and the uncertainty in the signal selection efficiency is 10% (20%) for the cut-based analysis (NN analysis). The largest contributions to the systematic uncertainties on the background are due to jet reconstruction efficiency (4.2%), jet energy scale (3.1%), background modeling (4%), and b -tagging efficiency (1.3%). For the signal, the systematic uncertainties stem from similar sources: jet energy scale

TABLE II. Summary of the analyses for a few $M(\rho_T)$ and $M(\pi_T)$ combinations. N_{obs} is the number of events observed in the data, N_B is the estimated background, ϵ_{sig} is the total efficiency for the signal. σ_{theory} is the theoretical prediction, while $\sigma_{\text{exp}}^{\text{limit}}$ and σ^{limit} are the expected and observed 95% C.L. upper limits for $\sigma(p\bar{p} \rightarrow \rho_T + X \rightarrow W\pi_T) \times BR(W \rightarrow e\nu)$, respectively, for $M_V = 500$ GeV.

$M(\rho_T, \pi_T)$ (GeV)	ϵ_{sig} (%)	N_{obs}	N_B	σ_{theory} (pb)	$\sigma_{\text{exp}}^{\text{limit}}$ (pb)	σ^{limit} (pb)
Cut-based analysis						
180, 90	2.7 ± 0.3	15	11.9 ± 0.9	1.24	0.92	1.22
185, 100	2.5 ± 0.3	10	7.5 ± 0.6	0.75	0.86	1.08
195, 100	3.3 ± 0.3	12	16.0 ± 1.2	0.95	0.82	0.58
205, 115	3.4 ± 0.4	9	10.1 ± 0.8	0.60	0.66	0.59
210, 110	3.8 ± 0.4	13	16.1 ± 1.2	0.70	0.72	0.56
Neural network analysis						
170, 85	3.8 ± 0.7	42	39.5 ± 9.8	1.2	0.77	0.95
175, 90	4.0 ± 0.8	36	35.6 ± 9.3	1.10	0.68	0.75
180, 90	3.6 ± 0.7	26	25.7 ± 7.8	1.24	0.66	0.82
205, 115	4.6 ± 0.9	20	21.7 ± 7.2	0.60	0.49	0.57
210, 110	4.3 ± 0.8	20	21.7 ± 7.2	0.70	0.53	0.60

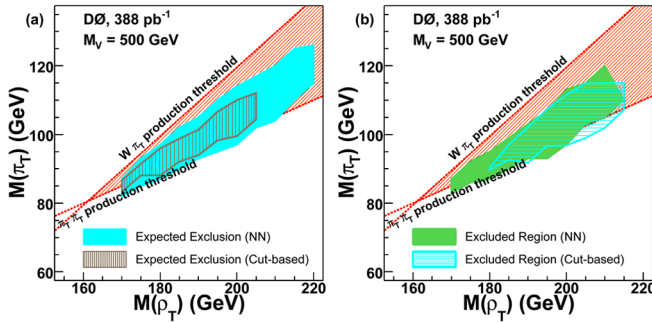


FIG. 2 (color online). Expected region of exclusion (a) and excluded region (b) at the 95% C.L. in the $M(\rho_T), M(\pi_T)$ plane for $\rho_T \rightarrow W\pi_T \rightarrow e\nu b\bar{b}$ production with $M_V = 500 \text{ GeV}$. Kinematic thresholds from $W\pi_T$ and $\pi_T\pi_T$ are shown on the figures.

(11.7%), jet resolution (9%), jet reconstruction efficiency (7.2%), b -tagging efficiency (6.5%), and from the difference between fast and fully simulated detector MC events (5.4%).

In the cut-based analysis, which is a simple counting experiment, we compute an upper 95% C.L. limit on the signal using Bayesian statistics [19]. The NN analysis performs a maximum likelihood fit of the data in the $M(\rho_T), M(\pi_T)$ plane to signal and background expectations. The backgrounds are constrained to their expected values within statistical and systematic uncertainties. The 95% C.L. upper limit on the signal cross section is then determined by the number of signal events below which lies 95% of the integral over the resulting likelihood function. In Table II, the limits for a few representative mass points are shown.

The expected sensitivity and the regions excluded at 95% C.L. by both analyses in the $M(\rho_T), M(\pi_T)$ plane for $M_V = 500 \text{ GeV}$ are shown in Fig. 2. Exclusion contour extends beyond the $\pi_T\pi_T$ production threshold because there is still some rate for $W\pi_T$ final state. For $M_V = 100 \text{ GeV}$, only a small region around $M(\rho_T) = 190 \text{ GeV}$ and $M(\pi_T) = 95 \text{ GeV}$ can be excluded. We note from Fig. 2(a) that the expected sensitivity of the NN analysis is better than that of the cut-based analysis, as indicated by the larger 95% C.L. exclusion region. We quote the observed 95% C.L. exclusion region in the $M(\rho_T), M(\pi_T)$ plane in Fig. 2(b) by the NN analysis as our measurement. (Consistent scaling of luminosity and background prior to optimization, using the new D0 luminosity [20], will lead to somewhat better limits. Nevertheless, we choose to keep the analysis consistent with the previous estimate of the luminosity value [11].) Although differences in the employed TC models, as stated in the introduction, preclude a direct comparison with previous searches [7], the current search achieves a higher sensitivity to the considered physics process.

We thank Ken Lane for helpful discussions, the staffs at Fermilab and collaborating institutions, and acknowledge support from the DOE and NSF (U.S.); CEA and CNRS/IN2P3 (France); FASI, Rosatom, and RFBR (Russia); CAPES, CNPq, FAPERJ, FAPESP, and FUNDUNESP (Brazil); DAE and DST (India); Colciencias (Colombia); CONACyT (Mexico); KRF and KOSEF (Korea); CONICET and UBACyT (Argentina); FOM (The Netherlands); PPARC (United Kingdom); MSMT (Czech Republic); CRC Program, CFI, NSERC, and WestGrid Project (Canada); BMBF and DFG (Germany); SFI (Ireland); The Swedish Research Council (Sweden); Research Corporation; Alexander von Humboldt Foundation; and the Marie Curie Program.

*On leave from: IEP SAS Kosice, Slovakia.

†Visitor from: Helsinki Institute of Physics, Helsinki, Finland.

- [1] S. Weinberg, Phys. Rev. D **13**, 974 (1976).
- [2] L. Susskind, Phys. Rev. D **20**, 2619 (1979).
- [3] S. Dimopoulos and L. Susskind, Nucl. Phys. **B155**, 237 (1979); E. Eichten and K. Lane, Phys. Lett. B **90**, 125 (1980).
- [4] K. Lane and E. Eichten, Phys. Lett. B **222**, 274 (1989).
- [5] K. Lane, Phys. Rev. D **60**, 075007 (1999).
- [6] K. Lane and S. Mrenna, Phys. Rev. D **67**, 115011 (2003).
- [7] T. Affolder *et al.* (CDF Collaboration), Phys. Rev. Lett. **84**, 1110 (2000); J. Abdallah *et al.* (DELPHI Collaboration), Eur. Phys. J. C **22**, 17 (2001).
- [8] K. Lane, *Technicolor 2000*, Lectures at Frascati Spring School (Frascati, Rome, 2000); arXiv:hep-ph/0007304.
- [9] V.M. Abazov *et al.* (D0 Collaboration), Nucl. Instrum. Methods Phys. Res., Sect. A **565**, 463 (2006).
- [10] G. Blazey *et al.*, in *Proceedings of the Workshop on QCD and Weak Boson Physics in Run II*, edited by U. Baur, R.K. Ellis, and D. Zeppenfeld (Fermilab, Batavia, IL, 2000), p. 47; see Sec. 3.5 for details.
- [11] T. Edwards *et al.*, Fermilab, Report No. FERMILAB-TM-2278-E, 2004.
- [12] T. Sjöstrand *et al.*, Comput. Phys. Commun. **135**, 238 (2001). We use PYTHIA version 6.224.
- [13] M.L. Mangano, M. Moretti, F. Piccinini, R. Pittau, and A.D. Polosa, J. High Energy Phys. **07** (2003) 001.
- [14] R. Brun and F. Carminati, CERN Report No. W5013, 1993 (unpublished).
- [15] L. Feligioni, Ph.D. thesis, Boston University [Fermilab Report No. FERMILAB-THESIS-2006-32, 2005 (unpublished)].
- [16] H.L. Lai *et al.*, Eur. Phys. J. C **12**, 375 (2000).
- [17] R. Hamberg, W.L. Van Neerven, and T. Matsuura, Nucl. Phys. **B359**, 343 (1991).
- [18] <http://schwind.home.cern.ch/schwind/MLPfit.html>.
- [19] I. Bertram *et al.*, Fermilab, Report No. FERMILAB-TM-2104, 2000.
- [20] T. Andeen *et al.*, Fermilab, Report No. FERMILAB-TM-2365-E, 2006 (to be published).